Author/s:
Dalic, LJ;Warren, AEL;Young, JC;Thevathasan, W;Roten, A;Bulluss, KJ;Archer, JS

Title:
Cortex leads the thalamic centromedian nucleus in generalized epileptic discharges in Lennox-Gastaut syndrome

Date:
2020-10

Citation:
Dalic, L. J., Warren, A. E. L., Young, J. C., Thevathasan, W., Roten, A., Bulluss, K. J. & Archer, J. S. (2020). Cortex leads the thalamic centromedian nucleus in generalized epileptic discharges in Lennox-Gastaut syndrome. EPILEPSIA, 61 (10), pp.2214-2223. https://doi.org/10.1111/epi.16657.

Persistent Link:
https://hdl.handle.net/11343/276318

DR. LINDA J. DALIC (Orcid ID : 0000-0001-8335-1348)

Article type : Full length original research paper

Title: Cortex leads the thalamic centromedian nucleus in generalized epileptic discharges of Lennox-Gastaut syndrome

Authors: Linda J. Dalic [1,2,3], Aaron E.L Warren [1,3,4], James C. Young[3], Wesley Thevathasan[1,5,6], Annie Roten[2], Kristian J. Bulluss[5,7,8], John S. Archer [1,2,3,4]

[1]*Department of Medicine (Austin Health) University of Melbourne, Heidelberg, Victoria, Australia.*

[2]*Department of Neurology, Austin Health, Heidelberg, Victoria, Australia.*

[3]*The Florey Institute of Neuroscience and Mental Health, Heidelberg, Victoria, Australia*

[4]*Murdoch Children's Research Institute, Parkville, Victoria, Australia.*

[5]*Bionics Institute, East Melbourne, Victoria, Australia.*

[6]*Department of Medicine, University of Melbourne, and Department of Neurology, The Royal Melbourne Hospital, Parkville, Victoria, Australia.*

[7]*Department of Neurosurgery, Austin Health, Heidelberg, Victoria, Australia.*

[8]*Department of Surgery, University of Melbourne, Parkville, Victoria, Australia.*

Corresponding author:

Dr Linda J Dalic

Austin Health, 145 Studley Road, Heidelberg, Victoria, Australia 3084.

Ph +61 3 9496 5000

Fax +61 3 9496 4065

Email – linda.dalic@austin.org.au

Running title: Cortex leads thalamus in Lennox-Gastaut syndrome

This is the author manuscript accepted for publication and has undergone full peer review but has not been through the copyediting, typesetting, pagination and proofreading process, which may lead to differences between this version and the Version of Record. Please cite this article as doi: 10.1111/EPI.16657

Key words: Thalamus, Deep brain stimulation, Generalized paroxysmal fast activity, effective connectivity, DBS, GPFA.

Text Pages: 18

Number of words: 3938/4000

Number of figures: 3

Number of tables: 2

Summary:

Objective –We aimed to assess the roles of the cortex and thalamus (centromedian nucleus; CM) during epileptic activity in Lennox-Gastaut syndrome (LGS) patients undergoing deep brain stimulation (DBS) surgery as part of the Electrical Stimulation of the Thalamus for Epilepsy of Lennox-Gastaut phenotype (ESTEL) trial.

Methods – Twelve LGS patients (mean age=26.8 years) underwent bilateral CM-DBS implantation. Intra-operatively, simultaneous EEG was recorded (range=10-34 mins) from scalp electrodes and bilateral thalamic DBS electrodes. Temporal onsets of epileptic discharges (generalized paroxysmal fast activity [GPFA] and slow spike-and-wave [SSW]) were manually marked on recordings from scalp (i.e., 'cortex') and thalamus (i.e., CM-DBS electrodes). Phase transfer entropy (PTE) analysis quantified the degree of information transfer from cortex to thalamus within different frequency bands around GPFA events.

Results – GPFA was captured in 8/12 patients (total event number across patients=168; cumulative duration=358s). 86% of GPFA events were seen in both scalp and thalamic

recordings. In most events (83%), onset occurred first at scalp, with thalamic onset lagging by a median of 98ms (interquartile range=78.5ms). Results for SSW were more variable and seen in 11/12 patients; 25.4% of discharges were noted in both scalp and thalamus. Of these, 74.5% occurred first at scalp with a median lag of 75ms (interquartile range=228ms). 1-0.5s and 0.5-0s before GPFA onset, PTE analysis showed significant energy transfer from scalp to thalamus in the delta (1-3 Hz) frequency band. For alpha (8-12 Hz) and beta (13-30Hz) frequencies, PTE was greatest 1-0.5s before GPFA onset.

Significance – Epileptic activity is detectable in CM of thalamus, confirming this nucleus participates in the epileptic network of LGS. Temporal onset of GPFA mostly occurs earlier at the scalp than in the thalamus. This supports our prior EEG-fMRI results and provides further evidence for a cortically driven process underlying GPFA in LGS.

Key words: Centromedian nucleus, Deep brain stimulation, Generalized paroxysmal fast activity, effective connectivity, DBS, GPFA.

Key points box:

- Simultaneous thalamic and scalp EEG during deep brain stimulation surgery shows generalised paroxysmal fast activity (GPFA) earlier at the scalp than thalamus.
- Phase transfer entropy analysis supports an initiating role for the cortex, with information transfer from scalp to thalamus prior to GPFA.
- Results provide further evidence that generalized epileptic activity of Lennox-Gastaut syndrome is initiated in the cortex and propagated through the thalamus.

Introduction

Lennox-Gastaut syndrome (LGS) is a severe, childhood-onset epilepsy associated with frequent seizures and intellectual disability. Although the causes of LGS are diverse, the electroclinical features are shared, likely reflecting epileptic recruitment of common neural networks that involve widespread brain areas including frontal and parietal cortex[1].

Tonic seizures and interictal generalized paroxysmal fast activity (GPFA) are key features of LGS. Both are characterised by diffuse low-voltage fast activity on scalp EEG, suggesting shared pathophysiological mechanisms. The generalized spatial extent of these events implies that synchronising structures in deep brain areas, in particular the thalamus, may play an important role. Indeed, previous studies using intracranial recordings from the human thalamus during generalized epileptic discharges demonstrated thalamic involvement in LGS[2, 3]; however, they did not clarify whether thalamic involvement is primary or secondary.

Using dynamic causal modelling (DCM) of simultaneous EEG-functional MRI (EEG-fMRI) data, we recently found evidence for a cortically driven process underlying GPFA in patients with LGS [4]. This approach suggested that GPFA is most likely initiated by prefrontal cortex, with propagation occurring first to the brainstem reticular formation and then from brainstem to thalamus [4]. Further evidence for a cortical initiator of epileptic fast activity in LGS comes from our observation that focal cortical lesions can produce a generalized LGS phenotype, whereas lesionectomy can abolish tonic seizures and GPFA[5, 6].

High frequency electrical stimulation (deep brain stimulation [DBS]) of the thalamic centromedian nucleus (CM) has been reported to modulate the occurrence of generalized seizures in LGS, with some patients experiencing significant seizure reduction[7]. Possible mechanisms underlying this modulatory effect include localised therapeutic influence of DBS upon pathological activity in the thalamus itself and/or downstream influences upon a more distributed set of cortical and subcortical areas connected to the thalamus[8].

In neuroscience, effective connectivity is defined as the influence that one neural system exerts over another[9] and can be used to evaluate the predisposition of neural pathways to propagate seizure activity[10]. Phase Transfer Entropy (PTE) is a recently introduced phase-based measure of effective connectivity that can estimate the frequency band-specific strength of information flow between pairs of brain regions[11]. It is based on the principle of

Granger causality[9] although is capable of handling non-Gaussian distributed variables making it well-suited to biological measurements such as EEG[12]. High PTE indicates strong effective connectivity (i.e., high directed influence of one region upon another) whereas low PTE indicates weak effective connectivity (i.e., low directed influence of one region upon another). Using PTE analysis, we recently found frequency-specific effective connectivity from piriform cortex to mediodorsal thalamus during absence seizures in a rodent epilepsy model[10].

In this study, we aimed to assess the relative roles of the cortex and thalamus (CM) in initiating epileptic activity characteristic of LGS. Intraoperative EEG recordings were acquired from both the thalamus and scalp during DBS surgery. Patients were studied as part of the Electrical Stimulation of the Thalamus for Epilepsy of Lennox-Gastaut phenotype (ESTEL) clinical trial. EEG recordings were first manually marked for epileptic event onset times. PTE analysis was then used to measure effective connectivity from scalp to thalamic electrodes, both prior to and during epileptic discharges within several frequency bands of interest. Given our prior EEG-fMRI work suggesting a driving role of the cortex in the initiation of GPFA in LGS[4], we hypothesised that (i) temporal onset of epileptic activity would occur earlier in EEG recordings from the scalp compared to the thalamus, and (ii) effective connectivity measured before and during epileptic events would show information flow in the direction of scalp to thalamus.

Methods

Patients

Twelve patients with LGS (mean age±1SD=26.8±5.7; 10 females) were recruited as part of the ESTEL trial of CM-DBS at Austin Health in Melbourne, Australia (Austin Health ethics approval HREC/16/Austin/139). Parents/carers provided written informed consent before patients entered a minimum three-month baseline observation period prior to DBS surgery. Confirmation of LGS diagnosis was made by two neurologists, requiring tonic seizures as well as EEG features of GPFA and SSW. Patient demographic information is presented in Table 1. Average age of seizure onset was 4.03 years, whilst the average duration of seizures prior to DBS surgery was 22.8 years. The causes of LGS were varied across patients and

included both genetic (*n*=4) and structural (*n*=3) etiologies; in five patients, cause of LGS was unknown.

DBS surgery including intra-operative EEG recordings

Each patient underwent bilateral CM-DBS electrode insertion using our previously described neurosurgical targeting approach [13]. Briefly, a Medtronic Activa® PC system with Medtronic model 3389 leads (4 x 1.5mm contacts on per lead; 0.5mm inter-contact distance) was implanted under stereotactic guidance (figure 1). The CM was identified pre-operatively on patients' 3T MRI scans using a Magnetisation-Prepared 2-Rapid-Gradient-Echoes (MP2RAGE) sequence that was processed using Sobel filtering to highlight intra-thalamic borders, together with a three-dimensional thalamic atlas[14] that was nonlinearly spatially warped to each patient's brain (for detailed methodological description, refer to Warren et al [13]). All surgeries were performed under a modified anesthetic regimen combining IV remifentanil (0.1-0.3 μg/kg/min) with inhalational isoflurane (0.5-0.7%). This anesthetic regimen was chosen because we have previously shown that it does not suppress epileptic discharges in patients with LGS and produces a scalp EEG similar to that seen during light natural sleep [4].

Intra-operatively, immediately following thalamic DBS lead insertion, and whilst still under anesthesia, all patients had simultaneous EEG recorded from the scalp and thalamus (mean recording length=23 mins; range=10-34 mins). CT-compatible scalp EEG electrodes (Rhythmlink® InvisaDeep Cup™) were placed in a modified 10-20 system which covered the temporal chains bilaterally, with midline and parasagittal electrodes omitted to permit surgical access. Thalamic recordings were obtained from thalamic DBS leads prior to connection of the Medtronic Activa® PC stimulator. Twelve hours pre- and post-operatively, patients had ambulatory scalp EEG recorded to confirm the presence of epileptic discharges.

Up to one day post-operatively, a volumetric CT scan was acquired to confirm accurate DBS electrode positioning. DBS lead trajectories were reconstructed by co-registering post-operative CT to pre-operative MRI scans using lead-DBS software version 2.1.8.1 [15]. Thalamic locations of DBS electrodes were determined by warping patients' CT-reconstructed lead trajectories to Montreal Neurological Institute (MNI) 152 2009b template

space, and then assigning each electrode to the nearest thalamic nucleus defined by the Krauth/Morel thalamic atlas [13, 14].

Identification of epileptic discharges on EEG

The EEG was displayed on a bipolar montage, with each thalamic (or scalp) contact referenced to an adjacent thalamic (or scalp) contact to avoid contamination of the EEG signal from signals distant from the recording location. Onsets and durations of epileptic discharges were marked manually at both scalp (presumed to represent adjacent cortex) and CM (i.e. thalamus) in both hemispheres. The EEGs were reviewed in detail by one epileptologist (LD) who analysed the record twice. A second, senior epileptologist (JA) reviewed a random selection of 50% of the manual mark-up to verify. The onset was defined as the first negative deflection seen on one or more EEG channels in either the scalp or CM electrodes; we did not require that all scalp or CM electrodes had epileptic activity at the onset point. Discharges <1s apart were classified as a single discharge train. Two groups of discharges were identified: (i) generalized fast activity (including both GPFA and electrographic tonic seizures; hereafter referred to as GPFA) and (ii) SSW (including both generalized and fragmentary SSW discharges). For each discharge that occurred in at least one or more thalamic and at least one or more scalp recordings, a 'lag time' (in ms; figure 2) was calculated by subtracting its earliest thalamic onset from its earliest scalp onset time (i.e. a positive lag time reflects an epileptic discharge that occurs first at the scalp, whereas a negative lag time reflects discharge occurrence first in the thalamus).

Effective connectivity measured using phase transfer entropy (PTE)

The strength of information flow from scalp to thalamus was estimated using PTE. PTE is the probability of the timing and phase of neural oscillations in one EEG recording source (in our case, a scalp electrode) predicting the timing and phase of neural oscillations in another EEG recording source (in our case, a thalamic DBS electrode) in a given frequency band of interest [11]. PTE is applied in the same fashion as real-value transfer entropy with the exception of the pre-processing transformation of data into an instantaneous phase signal [11]. When utilizing the Darbellay-Vajda adaptive partitioning algorithm, the input variables for PTE can be reduced to two input signals and a global time lag estimate in contrast to kernel density estimate approaches which require additional parameters (for details, refer to [10, 11]).

We chose to use PTE because (i) it provides frequency band-specific information concerning effective connectivity[11]; (ii) it has been shown to perform well in the presence of noise and non-Gaussian distributed measurements, which is typical of EEG[11]; and (iii) we have previously used this method to detect frequency-specific connectivity between cortical and thalamic EEG recordings of discharges in a rodent epilepsy model[10].

PTE analysis was performed for 7/8 patients who had intraoperative GPFA recorded in both CM and scalp/cortex; one subject (patient 2 in Table 1) in whom only two GPFA discharges were observed was excluded from the PTE analysis [10]. Frequency bands of interest were delta (0.5-3Hz), theta (4-7Hz), alpha (8-12Hz) and beta (13-30Hz). PTE analysis was not performed on SSW data due to large heterogeneity in EEG morphology and lag times for this discharge type, and due to the comparatively small number of SSW discharges in both scalp and thalamus that were captured per patient. To simplify analysis, we studied only right-sided contacts for each discharge in the CM (R electrode contacts C0, C1, C2, C3) and scalp EEG (Fp2, F8, T2, T4, T6).

For every identified discharge, PTE was measured in three **brain states**, each defined with respect to the discharge onset (figure 3): 'pre-onset' state (spanning -1 to -0.5s prior to discharge onset), 'onset' state (spanning -0.5s prior to discharge onset to the onset time defined as 0s) and 'event' state (spanning 0s to +0.5s post-onset). **Pathways** analysed were: Fp2→ R CM, F8→ R CM, T2→ R CM, T4→ R CM and T6→ R CM, where R CM was the EEG signal generated by only the subset of right-sided thalamic contacts that were confirmed by post-operative CT scans to be located within the CM [13] (figure 1).

For each frequency band of interest, we performed a two-way analysis of variance (ANOVA; implemented using the *anova2* function in Matlab version R2017b) testing for a main effect of each of the two independent variables 'brain state' (i.e., containing three levels: pre-onset, onset, and event) and 'pathway' (i.e., containing five levels: Fp2→ R CM, F8 → R CM, etc) on the dependent variable 'PTE', and their interactions. Significant main effects and interaction effects were tested at a threshold of $p<0.05$. Where a significant main effect was found, we performed post-hoc pairwise *t*-tests to explore PTE differences between brain states or pathways, with significance tested at $p<0.05$ (Bonferroni corrected for multiple comparisons).

Results

Manual analysis of epileptic discharge onsets on EEG

A total of 168 GPFA discharges were recorded from 8/12 patients (total duration of all GPFA discharges across patients=358.2s; mean duration per discharge±1SD=2.13±3.11s). Across the eight patients in whom GPFA was captured, the average number of GPFA discharges per patient was 21 (±1SD=10.5; Table 1). 86.3% (145/168) of GPFA discharges were observed in both one or more scalp electrodes and one or more thalamic electrodes. 12.5% (21/168) of GPFA discharges appeared in scalp electrodes only, while thalamus-only fast activity was noted for two discharges (1.2%).

Of the 145 GPFA discharges noted in both scalp and thalamic recordings, onset was observed earlier in scalp electrodes in 83.3% (140/168) of events, with thalamic onset lagging by a median time of 98msec (IQR=78.5msec). Per-patient mean lag time ranged from 75.13–138.87 ms (average±1SD=111.38±23.99; figure 2). Five discharges only were interpreted as having 'simultaneous' onset (i.e., their onsets were too close in time to be reliably differentiated by the EEG experts) in thalamus and scalp.

A total of 370 SSW discharges were recorded from 11/12 patients (total duration of all SSW discharges across patients=778.9s; mean duration per discharge±1SD=2.06±4.04s). Across the 11 patients in whom SSW was captured, the average number of discharges per patient was 33.6 (±1SD=19.7; Table 1). 70% (259/370) of SSW discharges occurred exclusively in scalp electrodes. 25.4% (94/370) of SSW discharges occurred in both scalp and thalamus: of these, 74.5% (70/94) showed onset earlier in scalp electrodes, with the thalamus lagging by a median time of 75msec (IQR=228msec). Per-patient mean lag time ranged from 17-1156 ms (average±1SD=223.23±330.75). Four discharges occurred first in the thalamus (median lag time=-60.5ms, IQR=-44.5). Scalp-only SSW was seen in 70% (259/370) of events, whilst thalamus-only SSW was noted in 4.6% (17/370).

Phase transfer entropy

PTE values varied within the four frequency bands analysed. The highest values, reflecting stronger effective connectivity from scalp to thalamic electrodes, were seen in the beta band, followed by alpha then theta bands, with the lowest PTE values observed in the delta band (fig.3A). There was an increase in PTE in the delta band prior to discharge onset, followed by a decrease in PTE in the delta and alpha bands during the actual event.

Results of the two-way ANOVAs are shown as an *F*-table in Table 2. For the delta, beta, and alpha frequency bands, we found a significant main effect of brain state on PTE values. We did not find any main effect of pathway, nor any interaction effects.

Post-hoc pairwise comparisons for brain state are shown in Figure 3B. We found: an increase in PTE in the onset state compared to the pre-onset state in the delta frequency band (p=0.038); a decrease in PTE in the event state compared to the pre-onset state in both the beta (p=0.039) and alpha (p=0.03) bands; and a decrease in PTE in the event state compared to the onset state in both the delta (p=0.004) and alpha (p=0.001) bands.

Discussion

Our study shows that the characteristic epileptic discharges of LGS occur earlier at the scalp (reflecting superficial cortical activity) than in deeper thalamic structures. Scalp EEG showed that GPFA occurs a median time of 98ms earlier than macro-electrodes placed directly within the centromedian nucleus of thalamus, implying bursts of cortical activity drive these 'generalized' discharges. Effective connectivity measurements with PTE provided supporting evidence, showing a direct influence of scalp/cortical regions upon the thalamus in the alpha and delta frequency band immediately prior to GPFA discharges. In contrast, the time lag between detection at the scalp and in the thalamus for SSW was more variable, implying that more complex interactions between cortical and subcortical structures may be involved in the initiation of this discharge type.

The finding that cortical involvement precedes thalamic participation in GPFA is consistent with our recent dynamic causal modelling (DCM) analysis of EEG-fMRI in LGS [4], which found that GPFA was more likely to be initiated by prefrontal cortex than either thalamus or brainstem. It is also consistent with our prior SPECT study of tonic seizures showing early blood flow changes in prefrontal cortex and the pontine region of the brainstem [16], and the

known phenomenon that cortical lesions can cause LGS whereas their removal can abolish seizures [5, 17]. Given our findings of widespread scalp EEG changes at GPFA onset, prior to thalamic involvement, it appears that mechanisms apart from the thalamus may be responsible for initiating epileptic activity across diffuse cortical regions. Alternatively, the thalamus may still participate at an early stage, but rather in setting the pre-requisite 'state' of an already unstable cortex, from which bursts of epileptic activity are then free to emerge.

This study confirms that the CM nucleus is involved during GPFA, but we cannot comment on other thalamic nuclei not sampled. Our prior EEG-fMRI studies of GPFA have shown maximal fMRI activation in anteromesial thalamic regions, particularly in the region of the mediodorsal and anterior thalamic nuclei [6]. However, the coarse spatial resolution of fMRI may not be sufficient to accurately assign activation patterns to specific thalamic nuclei. The CM has a functional role in sensorimotor coordination, cognition and pain processing, and has direct inputs to the striatum as well as to select cortical areas via the basal ganglia and other thalamic structures [18]. Its cortical connections include central and precentral cortex as well as anterior cingulate gyrus, a structure that is thought to be pivotal in seizure propagation [19]. Given these connections, it is not surprising that CM shows involvement in LGS. However, these data do not confirm whether or not the CM is a necessary component to sustain the epileptic network.

We found a temporal lag of approximately 100ms from the appearance of GPFA on scalp EEG to its appearance in the thalamus. This time delay is longer than what would be expected for direct transfer of an impulse from the cortex to the thalamus [20]. A possible explanation for this somewhat extended lag may be the time taken for neural activity to travel from cortical structures to the thalamus via indirect pathways, such as via the brainstem or basal ganglia [6] . In addition, scalp EEG and intra-thalamic recordings measure summed local field potentials, reflecting behaviour of local populations, rather than individual neuronal units. It is possible that thalamic delays in the EEG appearance of GPFA could represent additional time taken for a proportion or 'volume' of the local thalamic neuronal pool to exceed threshold to generate a measurable response. However, it is also possible the observed lag time may be an underestimate. Compared with intracranial electrodes, scalp EEG requires a larger neuronal pool to generate a response detectable by scalp EEG [21]. We cannot exclude the possibility that areas of cortex smaller than the detection threshold of scalp EEG begin firing first and setting off a GPFA burst, leading to an even greater lag to thalamic

involvement. In contrast, we can be fairly confident about the timing of firing in the CM, as this is a fairly small structure which we have sampled along its longest axis.

PTE estimates frequency-specific information transfer in the EEG signal between pairs of electrodes. Higher PTE values in the beta and alpha bands in the pre-onset state compared with the event state demonstrate that there is stronger effective connectivity within these bands prior to GPFA appearance on the EEG. A similar trend was seen in the alpha and delta bands, with peak PTE in the onset state compared with the event state. This demonstrates a causal influence of the cortex on the thalamus up to one second before discharge onset, and suggests a change in network properties that predispose the brain to GPFA occurrence. Lower PTE values seen *during* GPFA (i.e., in the event state) may reflect the loss of any temporal lag from cortex to thalamus due to the epileptic network entering a hyper-synchronous state.

The driving role of the cortex in development of other generalized epileptic discharges, including spike-wave discharges (SWD), has been demonstrated in animal models [22]. The time delay reported between sensorimotor cortical onset and thalamic appearance is often quoted in the magnitude of 500ms[23, 24] for SWD in rodent and feline models of Genetic Generalized Epilepsy. This represents more than a five-fold increase beyond the median thalamic lag times we observed here in patients with LGS of only 98ms during GPFA and 75ms during SSW. This discrepancy may reflect inherent differences between the epilepsy syndromes and models under investigation (i.e., human LGS vs animal models of Genetic Generalized Epilepsy), or perhaps methodological differences in discharge onset detection.

A small number of previous human studies have performed similar investigations of scalp versus thalamic onset times during epileptic discharges in patients undergoing CM-DBS implantation. In a group of six patients with various focal and generalized epilepsy types, onset times between scalp and CM appeared to vary according to the particular discharge type observed, with only spike-wave complexes originating from frontal scalp regions showing a reliably earlier onset time in scalp recordings compared to the thalamus [25]. In another study of four children with LGS, scalp and CM onsets were deemed to occur simultaneously during generalized tonic, tonic-clonic, and atypical absence seizures; however, the CM showed an earlier onset during myoclonic seizures only [2]. Conversely, a study of three patients (two with generalized epilepsy and one with frontal epilepsy)

determined that thalamic onset tended to lag cortical onset during generalized seizures in two patients; however, once the thalamus became involved, there was an increase in discharge rhythmicity consistent with a belated but then leading synchronising role of the thalamus[26]. Additionally, there was evidence of a thalamic lag in seizures arising from the frontal lobe[26], in keeping with our observations of GPFA, a discharge type that tends to show maximal amplitude over frontal and frontocentral scalp areas [27]. Variability in these previous studies' findings likely reflects heterogeneity in the epilepsy syndromes/seizure types studied, as well as small sample sizes.

We did not observe GPFA in four patients' intraoperative recordings. An overnight ambulatory EEG recording obtained <12 hours prior to surgery confirmed the presence of GPFA on the EEG of these patients, consistent with their diagnosis of LGS. Conversely, post-operative EEG obtained <12 hours following DBS electrode insertion in these four patients failed to demonstrate GPFA. Post-operative imaging confirms DBS electrode placement in the CM (figure 1) for all 12 subjects studied. We hypothesise that the absence of GPFA intra- and post-operatively in these four patients may be due to the microlesion ('implantation') effect of DBS surgery, which has been previously described[28-32]. Overnight EEG recorded three-months postoperatively (with stimulation off) confirmed re-emergence of GPFA, suggesting this implantation effect is a transient phenomenon. Whether the presence of an implantation effect predicts response to subsequent thalamic stimulation is yet to be determined. Other explanations for the lack of discharges include differences in recording length of EEG (and hence opportunity to capture events), anesthetic effects as well as inter-patient variation in the typical burden of discharges that occur on EEG.

Our findings are important considering the emerging development of responsive neurostimulation therapies for LGS. Responsive neurostimulators deliver electrical stimulation in response to user-determined parameters, including bursts of epileptic activity. In theory, our results suggest that stimulation may be better time-locked to bursts of epileptic activity if it is delivered in response to events detected from cortical structures as opposed to the thalamus. This may be particularly relevant to bursts of SSW, given we found that ~70% of these events were observed exclusively in scalp electrodes (and not also in thalamic contacts). However, it is unclear whether the ~100ms delay from scalp to thalamus is sufficient to affect efficacy. Given latencies involved in current seizure detection algorithms, this short delay may render stimulation prior to thalamic onset a technically challenging or

perhaps even impossible task. Our study also does not clarify whether stimulation will be most effective when it is delivered to brain areas showing the earliest onset of epileptic activity (this would favor a cortical stimulation approach in LGS), or when it is delivered to areas with widespread connections and broad neuromodulatory influence (this would likely favor a thalamic approach).

In summary, our intraoperative recordings of scalp and CM EEG suggest a leading role of the cortex in epileptic activity of LGS. GPFA appears earlier at the scalp than thalamus, with PTE results showing a directed influence of scalp-recorded cortical activity upon the thalamus that appears to occur prior to discharges. These results may have implications for the emerging development of responsive neurostimulation strategies to treat LGS. Once outcome data from the ESTEL trial are available, we will be able to assess whether the delay in GPFA or SSW correlates with seizure outcome after stimulation.

Acknowledgements

We thank the patients and their families and carers for participating in this research. Our work was supported with funding from the National Health and Medical Research Council (Project Grant #1108881). Linda J. Dalic is supported by an Australian Government Research Training Program Scholarship. Aaron E.L. Warren was supported by a post-doctoral fellowship from the Lennox-Gastaut syndrome Foundation and an Early Career Researcher Grant from the University of Melbourne.

Disclosure of Conflicts of Interest

Linda J. Dalic , Aaron E.L. Warren, James Young, Annie Roten and Kristian J. Bulluss report no conflicts of interest relevant to this study. John S. Archer has received honoraria from

Medtronic. Wesley Thevathasan has received honoraria from Medtronic and Boston Scientific.

We confirm that we have read the Journal's position on issues involved in ethical publication and affirm that this report is consistent with those guidelines.

References:

1. Archer JS, Warren AE, Jackson GD, Abbott DF. Conceptualizing lennox-gastaut syndrome as a secondary network epilepsy Front Neurol. 2014;5:225.
2. Velasco M, Velasco F, Alcalá H, Dávila G, Díaz-de-León AE. Epileptiform EEG Activity of the Centromedian Thalamic Nuclei in Children with Intractable Generalized Seizures of the Lennox-Gastaut Syndrome Epilepsia. 1991;32(3):310-321.
3. Velasco M, Velasco F, Velasco AL. Temporo-spatial correlations between cortical and subcortical EEG spike-wave complexes of the Idiopathic Lennox-Gastaut syndrome Stereotact Funct Neurosurg. 1997;69(1-4 Pt 2):216-220.
4. Warren AEL, Harvey AS, Vogrin SJ, Bailey C, Davidson A, Jackson GD, et al. The epileptic network of Lennox-Gastaut syndrome: Cortically driven and reproducible across age Neurology. 2019 Jul 16;93(3):e215-e226.
5. Warren AEL, Harvey AS, Abbott DF, Vogrin SJ, Bailey C, Davidson A, et al. Cognitive network reorganization following surgical control of seizures in Lennox-Gastaut syndrome Epilepsia. 2017 May;58(5):e75-e81.
6. Archer JS, Warren AE, Stagnitti MR, Masterton RA, Abbott DF, Jackson GD. Lennox-Gastaut syndrome and phenotype: secondary network epilepsies Epilepsia. 2014 Aug;55(8):1245-1254.

7. Velasco AL, Velasco F, Jimenez F, Velasco M, Castro G, Carrillo-Ruiz JD, et al. Neuromodulation of the centromedian thalamic nuclei in the treatment of generalized seizures and the improvement of the quality of life in patients with Lennox-Gastaut syndrome Epilepsia. 2006 Jul;47(7):1203-1212.

8. McIntyre CC, Hahn PJ. Network perspectives on the mechanisms of deep brain stimulation Neurobiol Dis. 2010 Jun;38(3):329-337.

9. Friston KJ. Functional and effective connectivity: a review Brain Connect. 2011;1(1):13-36.

10. Young JC, Paolini AG, Pedersen M, Jackson GD. Genetic absence epilepsy: Effective connectivity from piriform cortex to mediodorsal thalamus Epilepsy Behav. 2019 Aug;97:219-228.

11. Lobier M, Siebenhuhner F, Palva S, Palva JM. Phase transfer entropy: a novel phase-based measure for directed connectivity in networks coupled by oscillatory interactions Neuroimage. 2014 Jan 15;85 Pt 2:853-872.

12. Barnett L, Barrett AB, Seth AK. Granger Causality and Transfer Entropy Are Equivalent for Gaussian Variables. 2009.

13. Warren AEL, Dalic LJ, Thevathasan W, Roten A, Bulluss KJ, Archer J. Targeting the centromedian thalamic nucleus for deep brain stimulation J Neurol Neurosurg Psychiatry. 2020 Jan 24.

14. Krauth A, Blanc R, Poveda A, Jeanmonod D, Morel A, Szekely G. A mean three-dimensional atlas of the human thalamus: generation from multiple histological data Neuroimage. 2010 Feb 1;49(3):2053-2062.

15. Horn A, Li N, Dembek TA, Kappel A, Boulay C, Ewert S, et al. Lead-DBS v2: Towards a comprehensive pipeline for deep brain stimulation imaging Neuroimage. 2019 Jan 1;184:293-316.

16. Intusoma U, Abbott DF, Masterton RA, Stagnitti MR, Newton MR, Jackson GD, et al. Tonic seizures of Lennox-Gastaut syndrome: Periictal single-photon emission computed tomography suggests a corticopontine network Epilepsia. 2013;54(12):2151-2157.

17. Kang JW, Eom S, Hong W, Kwon HE, Park S, Ko A, et al. Long-term Outcome of Resective Epilepsy Surgery in Patients With Lennox-Gastaut Syndrome Pediatrics. 2018 Oct;142(4).

18. Ilyas A, Pizarro D, Romeo AK, Riley KO, Pati S. The centromedian nucleus: Anatomy, physiology, and clinical implications J Clin Neurosci. 2019 May;63:1-7.

19. Sadikot AF, Rymar VV. The primate centromedian-parafascicular complex: anatomical organization with a note on neuromodulation Brain Res Bull. 2009 Feb 16;78(2-3):122-130.

20. Magrassi L, Zippo AG, Azzalin A, Bastianello S, Imberti R, Biella GEM. Single unit activities recorded in the thalamus and the overlying parietal cortex of subjects affected by disorders of consciousness PLoS One. 2018;13(11):e0205967.

21. Tao JX, Baldwin M, Hawes-Ebersole S, Ebersole JS. Cortical substrates of scalp EEG epileptiform discharges J Clin Neurophysiol. 2007 Apr;24(2):96-100.

22. Beenhakker MP, Huguenard JR. Neurons that fire together also conspire together: is normal sleep circuitry hijacked to generate epilepsy? Neuron. 2009 Jun 11;62(5):612-632.

23. Meeren HK, Pijn JP, Van Luijtelaar EL, Coenen AM, Lopes da Silva FH. Cortical focus drives widespread corticothalamic networks during spontaneous absence seizures in rats J Neurosci. 2002 Feb 15;22(4):1480-1495.

24. Steriade M, Contreras D. Spike-wave complexes and fast components of cortically generated seizures. I. Role of neocortex and thalamus J Neurophysiol. 1998 Sep;80(3):1439-1455.

25. Velasco M, Velasco F, Velasco AL, Lujan M, Vazquez del Mercado J. Epileptiform EEG activities of the centromedian thalamic nuclei in patients with intractable partial motor, complex partial, and generalized seizures Epilepsia. 1989 May-Jun;30(3):295-306.

26. Martin-Lopez D, Jimenez-Jimenez D, Cabanes-Martinez L, Selway RP, Valentin A, Alarcon G. The Role of Thalamus Versus Cortex in Epilepsy: Evidence from Human Ictal Centromedian Recordings in Patients Assessed for Deep Brain Stimulation Int J Neural Syst. 2017 Nov;27(7):1750010.

27. Brenner RP, Atkinson R. Generalized paroxysmal fast activity: electroencephalographic and clinical features Ann Neurol. 1982 Apr;11(4):386-390.

28. Andrade DM, Zumsteg D, Hamani C, Hodaie M, Sarkissian S, Lozano AM, et al. Long-term follow-up of patients with thalamic deep brain stimulation for epilepsy Neurology. 2006 May 23;66(10):1571-1573.

29. Lim SN, Lee ST, Tsai YT, Chen IA, Tu PH, Chen JL, et al. Electrical stimulation of the anterior nucleus of the thalamus for intractable epilepsy: a long-term follow-up study Epilepsia. 2007 Feb;48(2):342-347.

30. Fisher R, Salanova V, Witt T, Worth R, Henry T, Gross R, et al. Electrical stimulation of the anterior nucleus of thalamus for treatment of refractory epilepsy Epilepsia. 2010 May;51(5):899-908.

31. Morrell MJ, Group RNSSiES. Responsive cortical stimulation for the treatment of medically intractable partial epilepsy Neurology. 2011 Sep 27;77(13):1295-1304.
32. Lane MA, Kahlenberg CA, Li Z, Kulandaival K, Secore KL, Thadani VM, et al. The implantation effect: delay in seizure occurrence with implantation of intracranial electrodes Acta Neurol Scand. 2017 Jan;135(1):115-121.

Table 1. *Clinical and EEG characteristics of 12 adults with LGS who underwent DBS surgery.*

Patient no/sex	Age at implantation (yrs)	Duration of epilepsy prior to surgery (yrs)	Duration of intraoperative EEG (min)	Types of intraoperative discharges recorded	Total GPFA discharges recorded (total duration [sec])	Total SSW discharges recorded (total duration [sec])
1/F	24	12	26	SSW	-	23(6.25)
2/F	18	15	17	SSW, GPFA	2 (17.7)	17 (7.05)
3/F	24	23.5	29	SSW, GPFA	18 (20.2)	68 (109.78)
4/F	30	25	26	SSW, GPFA	7 (2.6)	1 (1.0)
5/F	28	14	29	SSW, GPFA	27 (133.1)	57 (118.7)
6/F	28	27.7	34	SSW, GPFA	23 (19.4)	28 (44.37)
7/F	37	34.5	18	-	-	-
8/F	35	34	14	SSW	-	24 (9.0)
9/M	24	20	10	SSW, GPFA	33 (51.5)	34 (158.56)
10/M	31	30.8	25	SSW	-	24 (165.57)
11/F	20	15	19	SSW, GPFA	31 (12.2)	39 (23.23)
12/F	23	22.3	31	SSW, GPFA	27 (61.5)	55 (135.41)

Abbreviations: F, female; GPFA, generalized paroxysmal fast activity; M, male; SSW, slow-spike wave.

Table 2. *F-table showing main effects and interaction effects of brain state and pathways for PTE values associated with GPFA events across four frequency bands (delta, theta, alpha and beta; *=p<0.05).* In the delta, alpha and beta frequency bands, there is a significant effect of 'brain state' (i.e., the time windows before and during GPFA: 'pre-onset', 'onset' and 'event') on PTE values. However, we did not find an effect of 'pathway' (i.e., different pairs of scalp and thalamic electrode contacts) on PTE values, nor an interaction between brain state and pathway.

Frequency Band	*Source of variations*	*Sum of squares*	*Degrees of freedom*	*Mean square*	*F-score*	*p-value*
Delta (0.5-3 Hz)	Brain state	0.752	2	0.376	6.063	0.003*
	Pathway	0.143	4	0.036	0.575	0.681
	Interaction	0.036	8	0.005	0.073	1.000
	Error	5.579	90	0.062	-	-
	Total	6.509	104	-	-	-
Theta (4-7 Hz)	Brain state	0.013	2	0.007	0.592	0.556
	Pathway	0.015	4	0.004	0.344	0.848
	Interaction	0.005	8	0.001	0.057	1.000
	Error	1.007	90	0.011	-	-
	Total	1.041	104	-	-	-
Alpha (8–12Hz)	Brain state	0.231	2	0.115	7.178	0.001*
	Pathway	0.022	4	0.006	0.346	0.846
	Interaction	0.014	8	0.002	0.110	0.999
	Error	1.446	90	0.016	-	-
	Total	1.713	104	-	-	-
Beta (13-30Hz)	Brain state	0.298	2	0.149	3.640	0.030*
	Pathway	0.295	4	0.074	1.802	0.135
	Interaction	0.050	8	0.006	0.153	0.996
	Error	3.683	90	0.041	-	-
	Total	4.326	104	-	-	-

FIGURE CAPTIONS

Figure 1: Localization of DBS electrodes implanted into the thalamic centromedian nucleus (CM) for all twelve patients with LGS. (A) Bilateral quadripolar DBS electrode lead (Medtronic 3389) reconstructions based on postoperative CT scans for all patients (*n*=12), shown separately for the left and right CM (indicated by the shapes in yellow; these were derived from the three-dimensional Krauth/Morel thalamic atlas [14]). A sagittal view is provided for each brain side, as indicated by the directional arrows in the bottom left corner of each image (A=anterior direction; P=posterior direction; S=superior direction; I=inferior direction). Lead reconstructions were performed using lead-DBS software [15]. **(B)** Schematic showing lead width, contact size, and inter-contact distance for the Medtronic 3389 model. Each lead has four stimulation contacts (C0, C1, C2, and C3) spaced 0.5 mm apart. **(C)** Thalamic localisation of each right-sided lead contact (R C0, R C1, for all patients (*n=12*). Boxes shaded in yellow indicate electrode contacts located within the CM, as determined by the Krauth/Morel atlas [14]. (PF=parafasicular nucleus; VPM=ventral postero-medial nucleus; CM=centromedian nucleus; VL=ventrolateral nucleus; CL=central lateral nucleus).

Figure 2: GPFA and SSW discharge onset in CM relative to scalp during intraoperative EEG recordings. (A-B) Box plots showing the lag times (ms) of each GPFA (fig. 2A) and each SSW (fig. 2B) discharge (black circles), plotted per patient (y-axis). GPFA was observed in 8/12 patients (fig. 2A) and SSW observed in 11/12 (fig. 2B) patients undergoing DBS insertion. A positive lag time (i.e., a black circle to the right of the dotted zero line) indicates a epileptic discharge occurring first in the scalp EEG, whereas a negative lag time (i.e., a black circle to the left of the dotted zero line) reflects occurrence firstly in the thalamic CM. A lag time of zero (i.e., black circle on the dotted zero line) reflects occurrence of epileptic discharge occurring simultaneously in scalp and CM recordings. Across all patients and all discharges, the median lag time for GPFA was 98msec (IQR 78.5msec) and for SSW was 75msec (IQR 228msec). For each patient separately, the lower and upper ends of each box correspond to the first and third quartiles (i.e., spanning the inter-quartile range [IQR]) of lag times, respectively, while the middle horizontal line indicates the median. The lower and upper whiskers extend to the smallest and largest values no further than 1.5 times the IQR below the first quartile and 1.5 times the IQR above the third quartile. **(C-D)** Intraoperative

simultaneous scalp EEG (right-temporal chain) and right thalamic (quadripolar Medtronic model 3389 leads: R C0, R C1, R C2, R C3) EEG under anesthesia, shown for two example patients: patient 5 (fig. 2C) and patient 13 (fig. 2D). Onset of GPFA is usually earlier in the cortex (scalp) than in the thalamus, whereas onset of SSW is more variable.

Figure 3: Phase transfer entropy (PTE) values calculated for brain states prior to and during GPFA discharges in seven patients. (A) Line graph showing mean PTE values for each frequency band (delta, theta, alpha and beta) in the pre-onset (i.e., -1s to -0.5s prior to the GPFA onset time of 0s), onset (i.e., -0.5s to GPFA onset; shaded light-grey) and event (first 0.5s of the GPFA event; shaded dark-grey) brain states. Higher values of PTE reflect stronger effective connectivity in a given frequency band from scalp to thalamic regions. Error bars indicate 95% confidence intervals. **(B)** P-values (Bonferroni-corrected for multiple comparisons) for the post-hoc pairwise comparisons of PTE between different brain states in each frequency band.

A. Left and Right DBS lead positions (*n*=12)

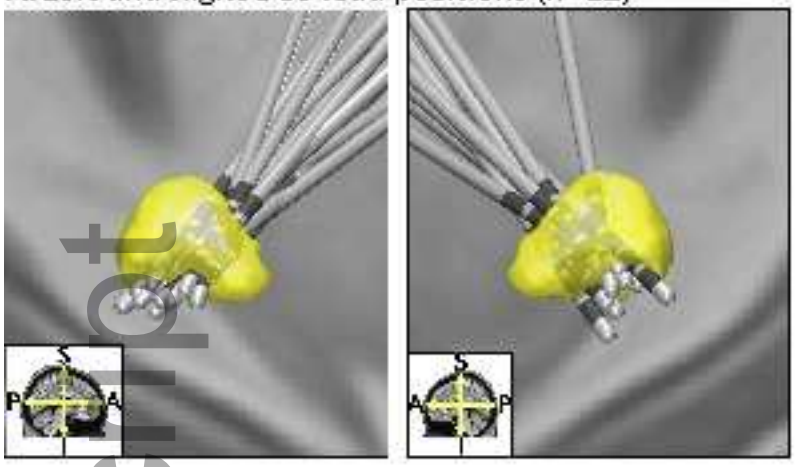

B. DBS electrode

C. Location of right DBS electrodes (*n* = 12)

PATIENT NO.	R C0	R C1	R C2	R C3
2				
3				
4				
5				
6				
7				
8				
9				
10				
11				
12				

epi_16657_f1.tiff

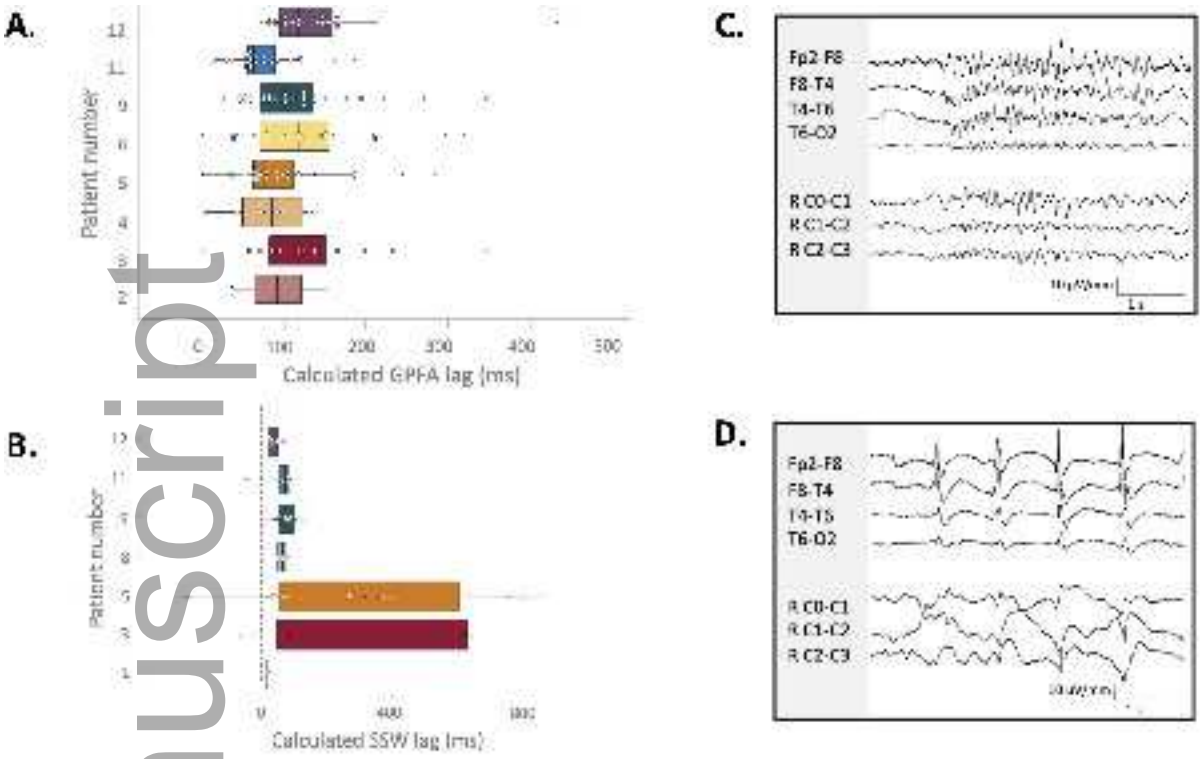

epi_16657_f2.tiff

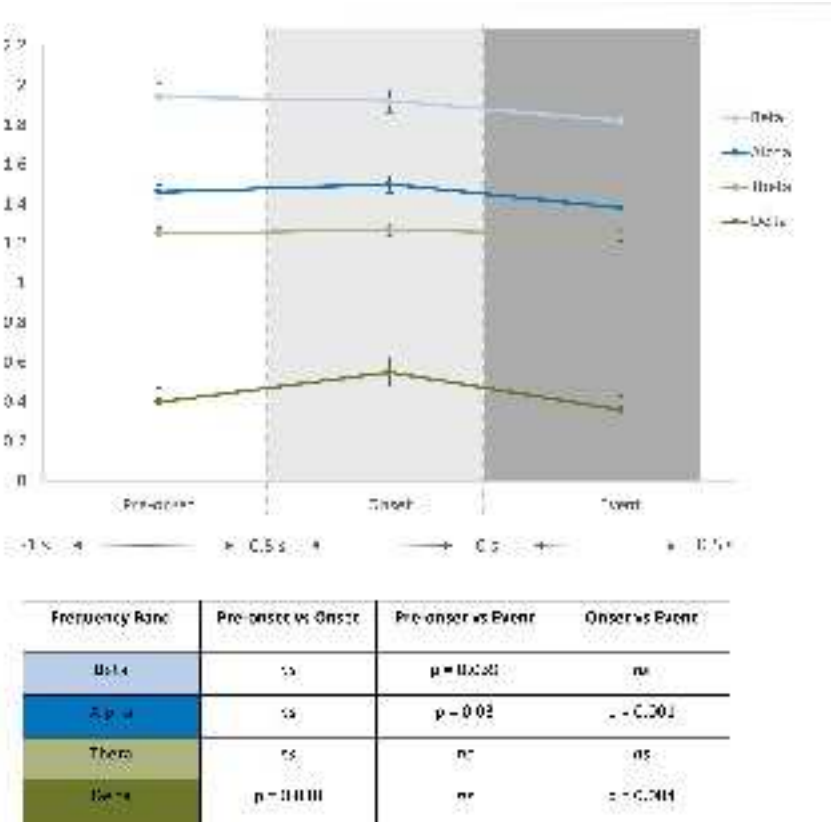

epi_16657_f3.tiff